Interpretation of the results of Static Load Tests on PLLN experimental piles

Miguel Ângelo Pedrosa Duarte
miguel.pedrosa.duarte@ist.utl.pt
Instituto Superior Técnico – Universidade de Lisboa, Lisboa, Portugal
Janeiro 2021

ABSTRACT

The analysis of static load test is nowadays essential to understand the behaviour of piles and are there many authors trying to describe its behaviour under theoretical models. Realizing the challenge that is describing its behavior only by theoretical models, on this thesis are described and analysed numerical an experimental model of driven and bored piles on the from Lisbon North logistics platform (PLLN).
Facing the importance of the numerical model on the design of such structures, it was analyzed one model for each pile using PLAXIS 2D software. On this kind of problems, it is essential to appreciate the role of the model's interface and understand how it can influence the results.
The classification of the soil is obtained by use of simple tests as standard and cone penetration tests. The numerical models are then compared to the theoretical and experimental models. Although the load-displacement curves it is still possible to optimize the models, mostly for the unloading part. The bored pile reproduced quite well the model. However, the driving pile showed to be tough to reproduce, demonstrated all the complexity that it contains.

1. INTRODUCTION

Planning a Civil Engineering project requires multiple efforts to provide a budget for a safe and in-time project deployment. Therefore, assessing the project requirements and risks is of primordial importance. One of the most crucial phases of the planning is the analysis of the soil's properties. In this thesis, we explore the theory behind driven and bored piles. These are two commonly used solutions, in many civil engineering works, to support heavy loads, mostly when the structure is founded on soft soils. To better understand the load transfer mechanism, it will be explained the bearing capacity.
This Thesis was developed to further explore the theory behind both driven and bored piles and reach numerical approximation, based on situ-test, as well as theoretical analysis. To validate the numerical use, it will be explored one example for each pile by use of the software PLAXIS 2D. The it will be analysed the case study of Lisbon North logistics platform, by describing the geotechnical area and then by performing numerical and theoretical approximations to compare with the experimental results and perform its analysis.

2. BEHAVIOUR OF A SINGLE PILE UNDER AXIAL COMPRESSION

2.2. Pile Types

In this chapter are introduced some of the many types of piles that are used in many construction projects and it will be explained some major differences between them. Then, it is explained the theoretical expression to evaluate its resistance. In this chapter are also explained some theories for the pile's toe bearing capacity and its failure surface.

Depending on its construction method, piles can be divided in two different groups: "displacement" and "non-displacement" piles. In the displacement piles there is no removal of soil, since it is displaced radially and axially, as the pile is inserted into the ground. In the non-displacement piles, the soil is excavated and extracted by an auger while being replaced/confined or not. The displacement piles groups can be divided on two groups (Fleming 2008), the low displacement piles that are usual small cross section like pipes and

H or I section piles and, the others that induces larger displacements and can be performed by caving a prefabricated pile or by using an auger that displaces the soils radially and axially.

2.2. Bearing Capacity of a Pile

In both piles, the total resistance can be evaluated by the sum of the shaft (R_s) and base resistance (R_b) [1].

$$R = R_b + R_s \qquad [1]$$

Both parameters are divided in terms of base resistance per are (q_b), base area (A_b), cohesion (c'), total and effective vertical stress at the base (σ_0 and σ'_0), end-bearing capacity factors for shear stress angle, rugosity of the pile's base and profundity effects (N_c, N_q and N_γ, being the last one neglected by Fleming (2008)), lateral resistance per area (q_s), adhesion coefficient (α), impulse coefficient (K), friction angle on the soil-pile interface (δ) and by the average vertical stress (σ_v). This results on the eqs. [2] and [3]:

$$R_b = q_b * A_b = (c' * N_c + \sigma_0 * N_q + \gamma * b * N\gamma) * A_b \qquad [2]$$

$$R_s = q_s * A_s = (\alpha * c' + K * tg(\delta) * \sigma_v) * A_s \qquad [3]$$

Although the formula presented for base resistance eq. [2] is quite used by the scientific community, the value of the factor N_c is still matter of discussion. For the factor N_q it is usual to adopt a value of 9 (Santos, 2008).

The following authors propose different theories for the value N_c

2.3 Terzaghi

Terzaghi suggest a theory based on the definition of the logarithmic arc CD (Fig. 1) by assuming ϕ' instead of α = π/4 + ϕ'/2, as some authors would consider (Santos 2008).

This results on a expression for N_c equal to:

$$N_q = tan^2\left(\frac{\pi}{4} + \frac{\phi'}{4}\right) * e^{\pi * \tan\phi'} \qquad [4]$$

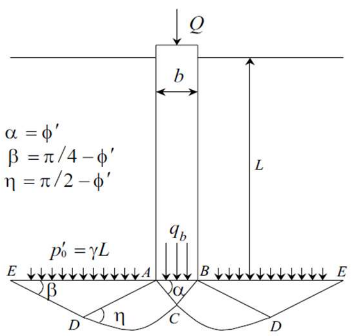

Figure 2- Terzaghi Slip Surface

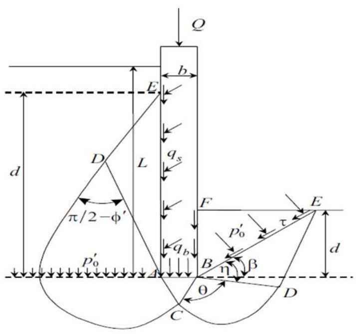

Figure 1- Meyerhof Slip Surface

2.4. Meyerhof

Meyerhof (1951) assumes that soil has the same properties above its base and so it can contribute for the bearing capacity of the pile's toe attributes the capacity to remain in an elastic equilibrium condition and acting as part of the foundation to the triangle ABC (Fig. 2). Meyerhof proposes different formulas accounting the Mohr diagram, the Mohr Coulomb failure criteria and a factor m (0 < m < 1) that characterizes the amount of shear strength that is mobilized on the equivalent free surface.
The value of the Nc can vary between the values when m=0 (Eq. [5]) and when m=1(Eq. [6]).

$$N_q = \frac{(1+\sin(\phi')) * e^{2\pi * \tan(\phi')}}{1-\sin(\phi')}$$ [5]

$$N_q = \frac{(1+\sin(\phi')) * e^{2(5/4\pi - \phi'/2) * \tan(\phi')}}{1-\sin^2(\phi')}$$ [6]

2.5. Berezantzev, Khristoforov and Gulubkov

Berezantzev et al. (1961) assumes that the soil that is displaced both in radial and axial directions and that forms compacted zones of soil in the surrounding area and that it has a huge effect in the bearing capacity of a pile. The soil's mass resulting from the radial compaction settles the same way as the pile, along the same length (L) with an internal radius that goes from A to B, where the height of that mass starts to be supported by frictional tension developed at the radius B (Fig. 4). The authors propose the Eq. [7] for the pile bearing capacity, where tha value Ak and Bk are obtained from Fig. 3 and the value of σ_0 is obtained according to Eq. [8].

$$q_b = A_k \Upsilon b + \sigma_0 B_k$$ [7]

$$\sigma_z = \frac{\tan\left(\frac{\pi}{4} - \frac{\phi'}{2}\right)}{\lambda_1 - 1} * \left\{ 1 - \left[\frac{1}{1 + \frac{\tan\left(\frac{\pi}{4} - \frac{\phi'}{2}\right)}{l_0} * \frac{z}{l_0}} \right]^{\lambda_1 - 1} \right\} \Upsilon l_0$$ [8]

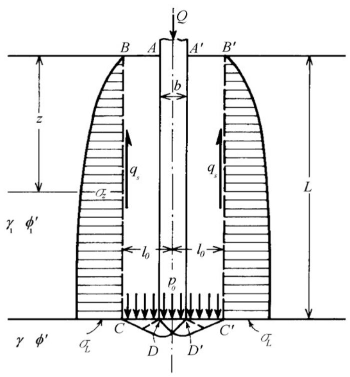

Figure 3- Berezantzev et al. slip surface.

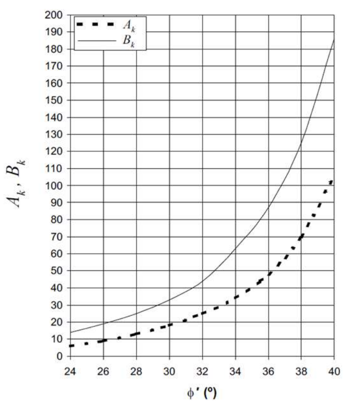

Figure 4- Values of A_k and B_k,

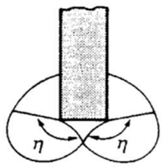

Figure 5- Janbu Slip Surface.

2.6. Janbu

Santos (2008) presents the equation to evaluate Nq, according to Janbu (1976). This new equation considers a slip surf as it is shown in Fig. 5 and Eq. [9], where angle η have a value between 70º and 105º if it is a soft clay or a dense sand, respectively. A higher value for η results automatically in a higher value for N_q and, consequently, increasing the bearing capacity of the pile.

$$Nq = \left(\tan(\phi') + \sqrt{1 + tan^2(\phi')}\right)^2 e^{2\eta \tan(\phi')}$$ [9]

3. NUMERICAL VALIDATION OF ELASTOPLASTIC MODELLING OF A SINGLE PILE UNDER AXIAL LOAD

In this chapter it will be discussed the many parameters involved in a numerical analysis using the PLAXIS 2D software and some comparisons will be done between the models provided by Ribeiro (2013) and the soil behaviour modulation properties from when a pile is driven into the soil proposed by Angelino (2015). This will allow to discuss the many properties that are involved in such exercise.

3.1. Interface and loading properties

Ribeiro (2013) applied a force on a generic model and between base load on the centre, base load on the side, distributed load, and prescribed displacements. It was observed that the prescribed displacements get closer to the real generation of stresses on the pile's head.

The initial horizontal stress ($\sigma'_{h,0}$) is calculated by using K_0, where K_0 stands for lateral earth pressure coefficient, and its relationship with the initial vertical stress (σ'_0) is showed on Eq. [10]

$$\sigma'_{h,0} = \sigma'_0 * K_0 \quad [10]$$

The value of K_0 can be calculated by three different forms: the K_0 procedure, the gravity loading and Field Stress procedure, that will not be a matter of discussion in the current document. The K0 procedure considers the already referred stress history of the soil and it can only have one value. This value of K_0=K_{0x}=K_{0y}, according to PLAXIS's manual, is based on Jaky's empirical formula (Eq. [11]).

$$K_0 = 1 - \sin\phi \quad [11]$$

When generating stress using this procedure, PLAXIS will generate vertical stresses that are in equilibrium with the self-weight of the soil and the horizontal initial stresses are calculated by using the value of K_0 for each type of soil. this procedure is recommended to use when the model has on its design only horizontal layers and phreatic level
The Gravity Load procedure calculates the initial stress based on volumetric weight of the soil and, when selected, its self-weight will be the first thing to be applied. This approach takes major importance when using a perfectly-plastic soil model such as the Mohr-Coulumb, where the value of the lateral earth pressure coefficient is highly dependent on the value of Poisson's ratio (ν) and, the value of K_0 is obtained according to the following expression:

$$\sigma'_{h,0} = \sigma'_0 * K_0 \quad [12]$$

Towards to obtain the best response possible from the model it is important to define well the interface properties once it will be essential to understand the amount of load that is carried by the pile's shaft and the part of the load that goes directly to the pile's base. There are two different factors that are used to define the interface. The first one (Eq. [13]) is the interface's virtual thickness, an imaginary dimension that defines the properties of the interface. This parameter can be manually defined and the higher it is, more elastic deformations will appear on it. The second parameter is the strength reduction factor, R_{int} (Eq. [14]). parameter that defines the amount of the total resistance of the soil that is mobilized. The strength of each layer can be defined according to:

$$c'_{interface} = R_{int} * c'_{soil} \quad [13]$$

$$\tan\phi_{interface} = R_{int} * \tan\phi_{soil} \quad [14]$$

The value of R_{int} can go from 0,01 to 1 and it should be adopted according to the material and as it will be demonstrated, it have a huge importance on the pile's response.

3.2. Modelling Steps

The first stage of modelling is defining the type of model (an axisymmetric model with 15 nodes elements will be used on the next modulations), its geometry (10x20 m^2 model for this example), with the properties presented on the next table:

Table 1- Soil's properties

		L (m)	Material Model	Materyal Type	Y [kN/m3]	c' [kN/m3]	ϕ' (º)	Ψ' (º)	ν	k0	E [kN/m3]
Reinnforced Concrete	Pile	10	Linear Elastic	Drained	24.0	-	-	0	0.3	-	29x106
Soil	Layer1	6,3	Mohr - Coulomb	Drained	16.7	13	26	0	0.12	0.562	9150
	Layer 2	2	Mohr - Coulomb	Drained	18.8	12	23	0	0.12	0.609	13510
	Layer 3	2,8	Mohr - Coulomb	Drained	19.8	14	23	0	0.07	0.609	13570
	Layer 4	8,9	Mohr - Coulomb	Drained	20.0	17	23	0	0.05	0.609	19300

Around the pile should also be defined two refinement areas with value of three pile's radius for the mesh refinement that was defined to be with the most refinement as it is possible.
Related to the water and seepage options, it was left the Plaixs default, i.e., with all the

boundaries open to the water flow. To perform the calculation, it is also important to define the movement of the model boundaries, they should be fully fixed on bottom, horizontal fixed on the laterals and free on top.

3.3 Results

After the initial stresses, the model should simulate the pile's construction process. The part of soil where the pile will fit, will be replaced by the concrete material, with all the interfaces turned off. This will replicate the behaviour of the auger on the soil, implying that the soil around the pile will not be too much disturbed. Then, the interfaces should be turned on, once that in this case all interfaces have different properties than the soil, and the displacements are set to zero. The load/displacement can now be activated and the results from the model can be obtained

A value for Rint equal to 0,01, means that the resistance of the soil on its interfaces are only a residual value. The differences between the value presented by Ribeiro (2013) are not significant (but still different), as can be seen on Fig. 6. On the other side, the values given when the R_{int} is set to 1, are much lower values than the values obtained by Ribeiro (2013) and its comparison of values can be found on Fig. 7.

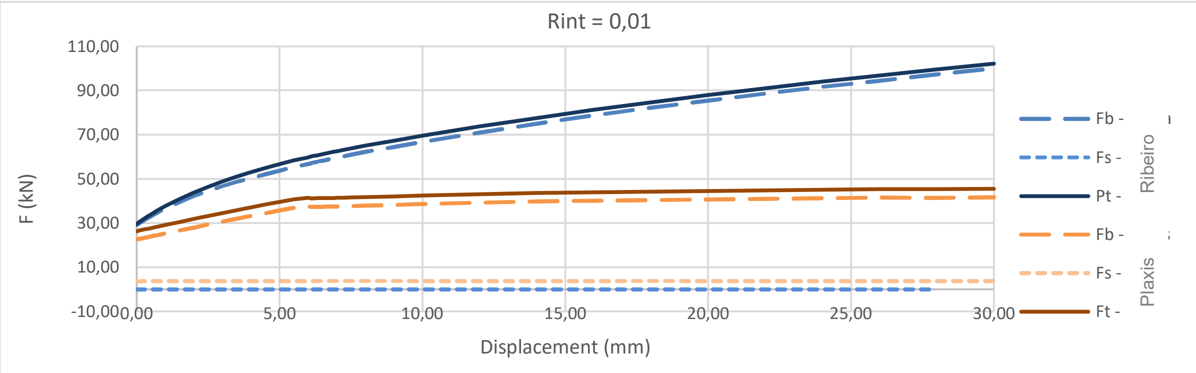

Figure 6- Comparation of between the values for Rint = 0,01.

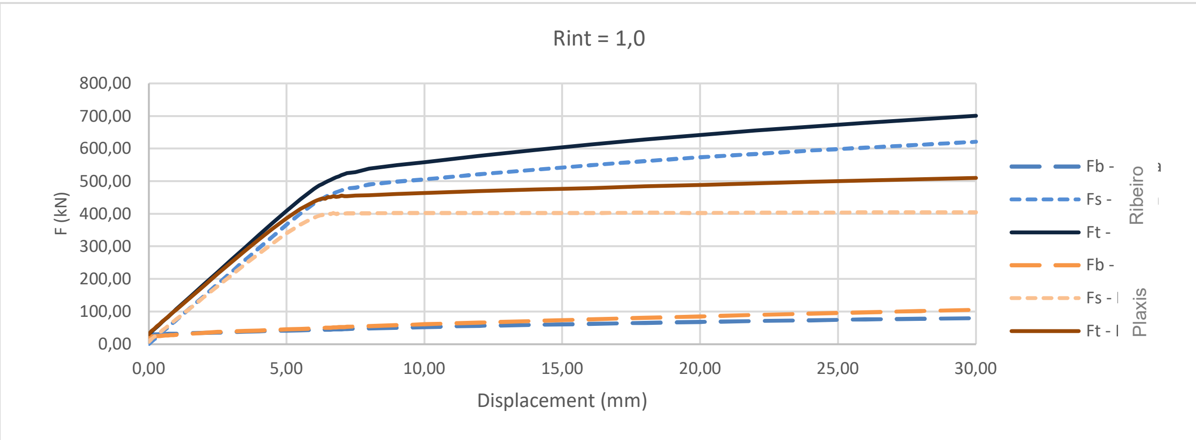

Figure 7- Comparation of between the values for Rint = 1,0.

It is perceptible the presence of an asymptote on the graph (Plaxis results), which indicates that even for a larger amount of displacement, the soil was not able to accommodate more load on its interface, meaning that the shaft resistance of the soil was already out of its capacity.

According to the equations 1 and 3, the soil's interface capacity describes very well that the results presented by Joana must have come from a model with stronger properties for some of its layers.

3.4. Driven Pile

The process of the pile's definition follows the same scheme than the bored pile model, However, as it was expected the process for the pile installation is different. As it was explained before on chapter 1, in this case, the soil where the pile will fit will not be removed and so the soil will be radially pushed so the pile can fit in it. To reproduce this process, Angelino (2015) simulates the process of displacement of the soil by removing the soil's area where the pile should fit and applying lateral pressure on the whole perimeter of the pile and on its bottom. These prescribed displacements are used to simulate the pressure that the ground applies on itself during this construction process. After this process of prescribed displacements, these are turned off and the empty area is activated with the concrete layer.

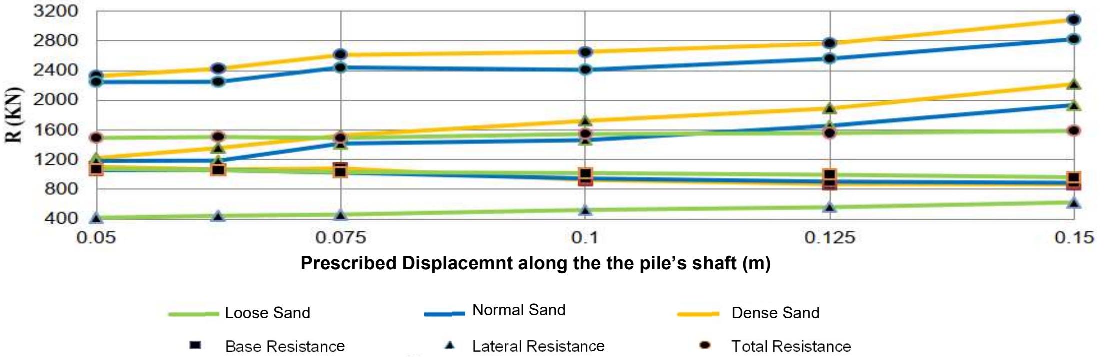

Figure 8- Resistance of the pile according to different prescribed displacements and different kinds of soil, for a 0,360m diameter pile. Adopted from Angelino (2015).

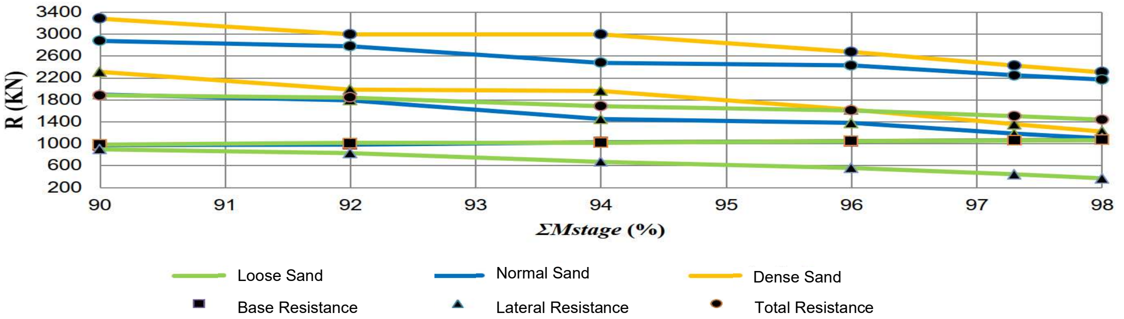

Figure 9- Pile's resistance with the variations of the multiplier $\sum M_{stage}$.

Although it is not certain the amount of displacement to be applied on, Angelino suggests doing it as an iterative process where the following variables will vary displacement at the bottom, lateral displacement and the PLAXIS variable, the $\sum M_{stage.}$ As shown on Fig. 8, the amount of lateral displacement prescribed on the soil will give a bigger value for soil resistance in its global, but the base resistance may reduce a bit. It is also possible to understand from the same image that the effect of soil prescribed displacement is more significant on dense sand.

The $\sum M_{stage}$ factor is a multiplier associated with the staged construction process. This factor allows the software to move to the next stage without ending the current one. When defines to a value lower than one, the ultimate level of the phase is not finished, and it will be ended on the following stage, although the following step have to be calculated as *Staged construction*. This tool allows to better control the process of removing the soil and the appliance of prescribed displacements without the soil's body collapse. This follows the same principle of the construction a NATM tunnel, where the forces around the empty hole are calculated by use of the expression (1-β)

4. Case Study - Lisbon North logistics platform (PLLN)

It is intended to build several warehouses to be working mostly as logistic centres at Lisbon north logistics platform (PLLN). This location is known to be part of the wetlands of Tagus River, being mostly composed by soft clays (reaching sometimes the 70 meters deep) and a high level of the water table therefore it is important to have a full definition of the behaviour of piles under axial loading.

4.1. Lithology and soil characterization

To characterize the indicated site, several tests as Boreholes for extraction of soil, Standard Penetration Tests (SPT) and Cone Penetration Tests (CPT) were performed to evaluate the properties of each layer of soil until the 40 meters deep.
By the bore hole is possible to identify 3 meters of embankment followed by almost 14 meters of muddy clay soil. From 17,40 to 19,5 it is showed some coarse silt sand followed by almost 5 meters of silty-sandy clay. At the 24 meters deep appears a 4-meter layer of fine to coarse sand that is interrupted at the 28 meters deep by a thin layer of mud with clay and fine sand. From the 30 meters the soil goes from fine sand to coarse sand
It was assumed that the Poisson Coefficient (ν) has a value of 0,3 for drained layers of soil and a value of 0,5 for undrained layers. By use of the equations proposed Liao & Whitman (1985), Bowles (1971), Terzaghi & peck (1967) and Kulhawy and Mayne (1990), it was possible to correlate the corrected number of blows $(N1)_{60}$, the unit weight (γ), the shearing resistance (C_u),

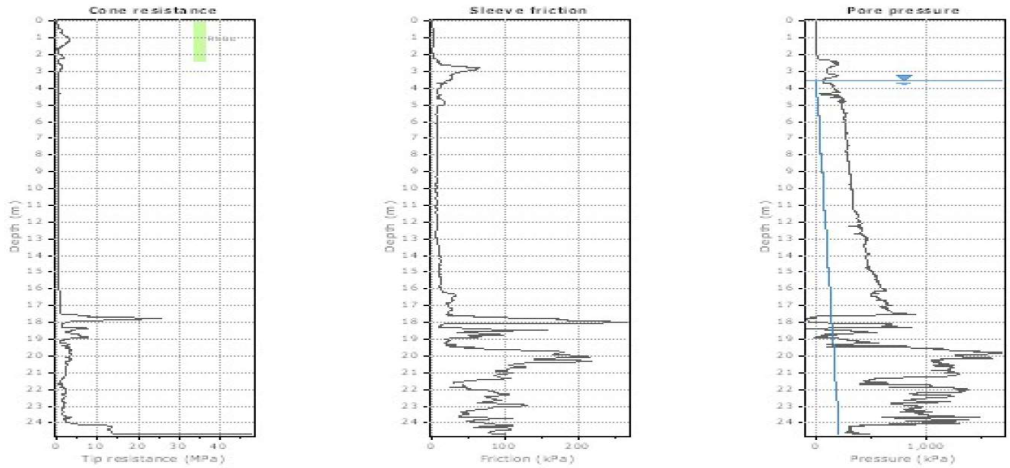

Figure 10- Variation of Base and Shaft resistance and pore water pressure (Mota Engil)

he angle for shear resistance (ø') and the elastic modulus (E), respectively.
However, the results provided by the Piezo-Cone Penetration test show to be more reliable since it allows to classify the soil continuously without any gaps, as the SPT does. Mostly by the adoption of Robertson (1990) for the type of soil represented on Fig. 10, it was possible to better estimate the soil properties that will be used on the numerical theoretical models.

4.2. Bored Pile

The 34m long and 800 mm diameter pile was tested with the set to reach 2 times its maximum capacity, 5600 kN. Since it was performed only eight days after its casting, the Elastic modulus was adjusted according to the Eurocode 2 expression:

$$E = E_{u,28d} * \sqrt{e^{s\left(1-\sqrt{\frac{28}{t}}\right)}} \quad [15]$$

From the data collected by the STL, it was possible to obtain the following load-displacement curves (Fig. 11).
The numerical model was performed using the parameter present on table 2.

Table 2- Numerical soil properties.

Layer	Material Model	L (m)	γ (kN/ m^3)	Cu (kPa)	Ø'(º)	E (MPa)	ν	R_{int}	K_0
1	Mohr–Coulomb	3	19	-	30	35	0,3	0,62	0,470
2	Mohr–Coulomb	12	15	30-60	-	5	0,499	0,8	1,0
3	Mohr–Coulomb	2	15	75	-	40	0,499	0,9	1,0
4	Mohr–Coulomb	2	20	-	32	70	0,3	0,640	0,441
5	Mohr–Coulomb	5	18	120	-	55	0,499	0,90	1,0
6	Mohr–Coulomb	10	21	-	36	130	0,3	0,62	0,412
Concrete	Linear Elastic	34	25	-	-	30 *10^3		1,0	1,0

Note that for this calculation, the interface was defined only by the parameter R_{int} and it was not defined any interface structure.
The water table was defined at 3,3 meters deep.

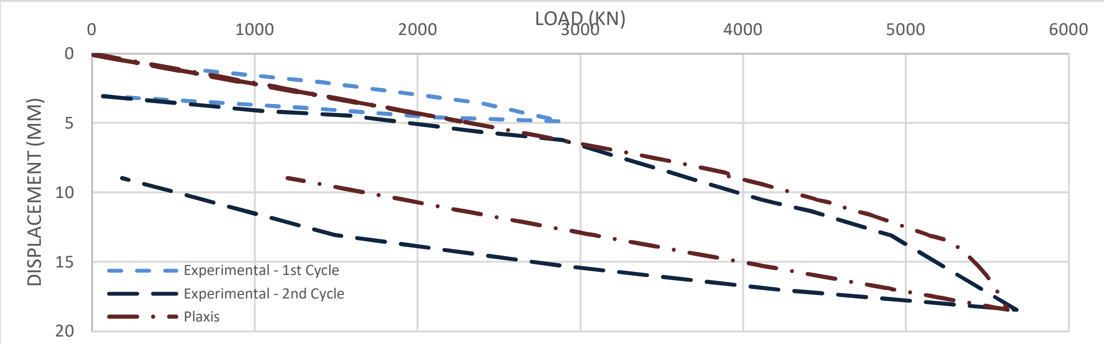

Figure 11- Bored Pile's Load-Settlement Curve.

On figure 11 it is represented the load-displacement curves form the numerical test and from the bored pile. However, to estimate the amount of load carried by the pile shaft, it was necessary to access the information provide by the extensometers installed all along the pile. When the maximum load is applied, the pile is carrying about 4600 kN. While the theoretical equations estimated to the maximum resistance to be 4499,9 kN. In a further numerical analysis, the pile was subjected to a fiction load leading to the collapse. The estimated total bearing capacity of the pile it was estimated to be 11.483 kN. By estimating the plastic base formation, it was associated the slip surface provided by the model to the failure surface proposed by Janbu. Although it hard to estimate, the lower slope of the experimental pile indicates that the bearing capacity may be higher than the one obtained by the numerical model, by the slope provided by the numerical model when load until its full capacity.

4.3. Driven Pile

The driven piled had square section of 400mm with 31.8 meters long, with a metallic connection between its segments. It was insert on the ground by use of an automatic hammer and right after its installation on the ground, a test based on wave propagation verified that the pile's integrity. The soil properties were left the same as the used before, with the only concern being about the pile interface that was used this time to reduce both strength and elastic properties to better simulate the process of craving a pile into the ground. And so, the R_{int} used was:

Table 3- Strength and Elastic reduction of the Driven Pile Interface.

	GZ1	GZ 2	GZ 3	GZ 4	GZ 5	GZ 6
R_{int}	0,40	0,9	0,8	0,7	0,8	0,5
E (MPa)	15	1	25	50	20	70

As showed on chapter 3, to simulate the introduction of the pile it was necessary to add load displacement structures. Although, unlike the model proposed by Angelino where he prescribes displacements over the model's interface at once, this time, the pile is introduced step by step so it can get closer to the real process of installation. It was adopted 10 steps to insert the pile

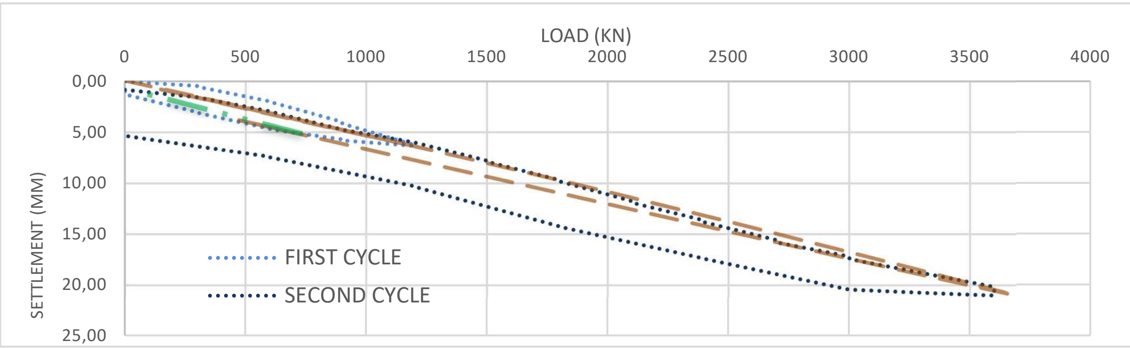

Figure 12- Load - Displacement curve of the Driven Pile SLT.

on the ground. All the displacements were put back to zero (like it was done on the bored pile model) so it was possible to obtain the displacement from the test.
The lateral displacement was defined to 0,035 m (0,07 D) and a base displacement of 0,15 m (0,3 D). The base's displacement showed to be determinant on the magnitude of the shaft resistance. When a lower displacement is applied on the pile's base the shaft resistance tends to get bigger. However, not matter how much or lower the value of the resistance gets, the soil's load – displacement curve does change, almost recovering to its initial state.
Leading the test to its ultimate capacity, it was possible to conclude that the bearing capacity of the pile on the numerical model is estimated to be 8000 kN. And, for that ad for the Plastic Point's formation on the model it is estimated that the Berezantzev theory estimates with more accuracy the bearing capacity of the driven pile.
Wen observing the decomposition of the load in the loads carried by the base and the pile tip (Figure 13), it may seem that both theories (Table 11) overestimate the results obtained by the pile. The negative force value on the craved pile shaft present on the Plaxis graph, once again, might be correlated to the construction process. Some authors have referred the existence of a residual load associated, more commonly, to driven piles.
Fellenius (2015) describes that during the last impact of hammer on the insertion of a driven pile into the ground it appears to be created a residual force on the pile is toe and along the pile is shaft. This imprisoned load is accentuated due to the consolidation that happens on adjacent soil after the pile's insertion.

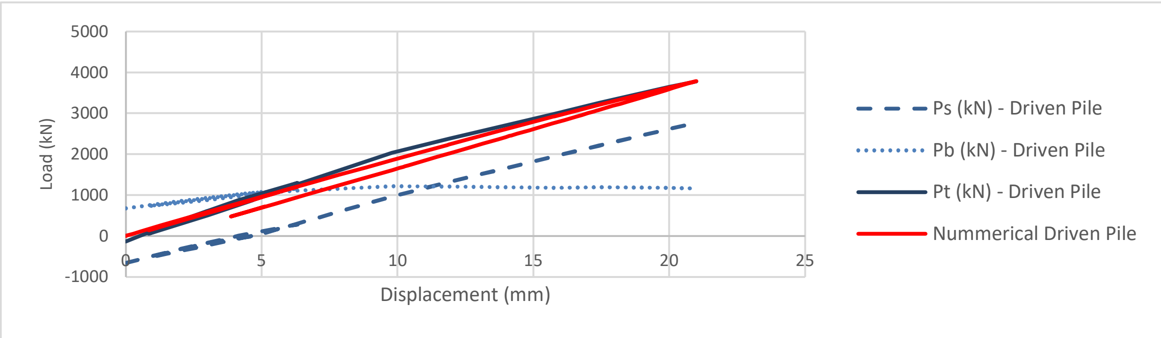

Figure 13- Decomposition of the total load on the driven pile.

As the Figure 13 indicates and as Figure 14 proves, the Plaxis model replicated that effect, with stresses appearing on the pile's base, creating a negative friction on the pile shaft, and the down drag effects are also present on the pile's upper body, although with a low value of positive shaft resistance mobilized when compared to the other.

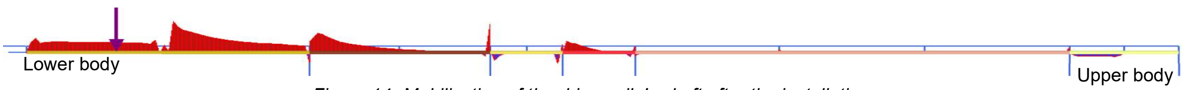

Figure 14- Mobilization of the driven pile's shaft after the installation.

4.4 Overall Remarks

The first remark that it important to stand is the enormous difference between the slopes corresponding to both displacement and bored piles. Something that would be expectable once the bored pile has twice the driven pile dimensions. Looking to the comparative values of the shaft strength mobilization:

Table 4- Comparative values between piles shaft resistance

	Shaft Mobilization			
	Total (kN)		Unitary (kN/m²)	
	Bored	Driven	Bored	Driven
Theoretical	4500	2822	52,66	56,53
Numerical	4436	2771	51,91	56,54
Experimental	4500	3000	52,66	60,10

We can see a higher mobilization of force on the driven pile shaft. The theoretical values show a lower difference since the difference stands only for their lengths and the role it takes to calculate the average value of vertical stresses on the last layer of soil. The difference gets bigger on the numerical and experimental models, where experiments take in account the construction process, and as the table shows, the differences between the theoretical value with the others are higher for the displacement pile. This may induce that those formulas are more accurate to piles that does not disturb the soil in same level as a displacement pile does.

5. CONCLUDING REMARKS

Although the results obtained were satisfactory since the numerical models estimated the shape of the experimental load-displacement curves and the theoretical methods proved to give good estimations of the bearing capacity of the pile, it is still important to refer some final notes:

On the second chapter:

- Although the equations proposed give a good estimative for both piles, they were formed based on empirical methods and so, some differences can be found from one model to another no matter how many cases proven to be right.

On the third chapter:

- Among the parameters mentioned (loading, lateral earth pressure and interface), the last one revealed to be the most significant one, with a huge role on the shaft resistance of the numerical model.
- Meanwhile, nor the dimensions of the model proposed, nor the refinement of the mesh had much influence on the results, at least for the design loads of the presented models.
- For the driven pile, the amount of axial displacement prescribed on the soil under the pile's toe, during the construction process, demonstrated to have a big influence on the amount of shaft resistance carried by the pile's shaft. On the other side, the definition of ∑Mstage, does not have a big influence on the results provided by the model. However, its definition is very important to prescribe the displacement without stopping the calculations of PLAXIS.

On the fourth chapter it is possible to conclude that:

- Besides the numerous data provided for the soil most simple tests (boreholes, SPT and CPTu), there exist some space for misunderstandings due the various correlations available nowadays and due to the empirical experience, that is also important for the soil classification. This leaves room for some discrepancies in the soil characterization values.
- The numerical approach and theoretical results matched well the curve load-displacement obtained from the experimental test. However, there is room to change and improve, at least in at the unloading phase, due to soil's almost perfect-elastic behaviour.
- In the bored pile numerical analysis, the interface structure showed to have not such importance as it was expected, however, it depends on the model and its iterative process for the soil properties.
- The driven pile showed itself to be the most difficult test to replicate in both numerical and theoretical models. The amount of soil's displacement and plasticisation is still hard to quantify and so the following analysis showed to fail in some points. The load-displacement curve is almost perfect-elastic, what does not match the experimental results. Also, the shaft resistance of the numerical analysis showed to have not reached its limit and so, it has overestimated the results provided for both numerical and theoretical solutions.

There still exists space to improve the results and to explore more both experimental tests and the major differences between those and the theoretical approaches.

- Note also that the value of the Elastic Modulus of the pile is not constant all over the test and so it should be estimated with more certainty in many steps so that the pile test can reproduce with more accuracy the results of the test.
- For last, the residual load showed to be essential on the interpretation of the static load test, it should be further analysed to improve the experimental result.

REFERENCES

A, Krasinski. Numerical simulation of screw displacement pile interaction with non-cohesive soil. Archives of Civil and Mechanical Engineering. Volume 14. Issue 1. Pages 122-133. 2014.

Alawneh, Ahmed Shlash et al. "Axial compressive capacity of driven piles in sand: a method including post-driving residual stresses". Canadian Geotechnical Journal 38. 2(2001): 364–377.

Angelino, João. Estacas de Deslocamento sob Ações Verticais. Instituto Superior Técnico. (2015). Tese de mestrado em Engenharia Civil, Instituto Superior Técnico, Universidade de Lisboa.

Ausweger, Mario & Binder, Eva & Lahayne, Olaf & Reihsner, Roland & Maier, Gerald & Peyerl, Martin & Pichler, Bernhard. Early-Age Evolution of Strength, Stiffness, and Non-Aging Creep of Concretes: Experimental Characterization and Correlation Analysis. Materials. 12. 207. 10.3390/ma12020207. (2019)

Berezantzev, V.G., and V.Alaroshenko (1962). Peculiarities of sand deformations under deep foundations. Bases, Foundations and Soil Mechanics, No. 1

Brinkgreve, R. B. (2006). Plaxis - 2D Version 8 Manual. The Netherlands: Delft University of Technology and Plaxis b. v

Bourne-Webb, P. (2019). Geotechnical Characterization. Presentation of the Special Foundations course (in Portuguese). Instituto Superior Técnico.

EN 1992-1-2, 2004. Eurocode 2: Design of Concrete Structures - Part 1-2. 1st ed. Brussels: BSi.

Fellenius, B. H. "Static tests on instrumented piles affected by residual load." DFI Journal-The Journal of the Deep Foundations Institute 9.1 (2015): 11-20.

Fleming, K. and Weltman, A. and Randolph, M. and Elson, K.. Piling Engineering, Third Edition. Taylor & Francis. (2008)Janbu, N. 1976. Static bearing capacity of friction piles. In Proceedings of the 6th European Conference on Soil Mechanics and Foundation Engineering, Vienna, Austria. Vol. 1.2, pp. 479–488.

Kulhawy, F.H. & Mayne, Paul.. Manual on Estimating Soil Properties for Foundation Design. (1990)

Liao, S.C. & Whitman, R.V. 1986. Overburden correction factors for SPT in sand. ASCE Journal of Geotechnical Engineering 112 (3):373-377.

MEYERHOF, G. G. Some recent research on the bearing capacity of foundations, Vol. 1 – n. 1 – 1963, 16-22 p.

Meyerhof, G. G. "The ultimate bearing capacity of foudations." Geotechnique 2.4 (1951): 301-332.

Mota-Engil Fundações. (2019). Memória Descritiva e Justificativa – Análise dos Reultados dos Ensaios de Carga Estática, Doc3187/DRC1/01-NT– Plataforma Logística de Lisboa Norte – Lote 19, Castanheira do Ribatejo.

Prandtl, L. (1920) "Über die Härte plastischer Körper." Nachr. Ges. Wiss. Goettingen, Math.-Phys. Kl., pp. 74–85.

Randolph, M., & Wroth, C. (1978). Analysis of Deformation of Vertically Loaded Piles. JGED, ASCE104(GT12), pp. 1465-1488

Ribeiro, J. (2013). Behaviour of single piles under axial loading: Analysis of settlement and load distribution. Tese de mestrado em Engenharia Civil, Instituto Superior Técnico, Universidade de Lisboa.

Robertson. P.. Interpretation of cone penetration tests - A unified approach. Canadian Geotechnical Journal. 46:1337-1355. (2009).

Robertson P.K., Cabal K.L. "Guide to Cone Penetration Testing for Geotechnical Engineering". Gregg drilling. 6th edition July 2015

Robertson, P. K., Campanella, R. G., and Wightman, A. 1982. SPT-CPT correlations. University of British Colum- bia, Civil Engineering Department, Soil Mechanics Series, No. 62, and ASCE Journal of the Geotechnical Division (accepted May 1983).

Santos, J. A. (2008). Fundações por estacas: Acções verticais. Elementos teóricos da unidade curricular de Obras Geotécnicas, Instituto Superior Técnico, Universidade de Lisboa, 25 p

Terazaghi, Karl. "Theoretical soil mechanics." John Wiley and Sons (1965).

Tjie-Liong, G. O. U. W. "Common mistakes on the application of Plaxis 2D in analyzing excavation problems." International Journal of Applied Engineering Research 9.21 (2014): 8291-8311.